Proceedings World Geothermal Congress 2015
Melbourne, Australia, 19-25 April 2015

Characterizing Surface Manifestation of Geothermal System under Torrid Zone using Synthetic Aperture Radar(SAR) Data

Asep Saepuloh, Arif Susanto, Prihadi Sumintadireja, and Emmy Suparka

Faculty of Earth Sciences and Technology, ITB, Jl. Ganesha No. 10 Bandung, Indonesia

E-mail:saepuloh@gc.itb.ac.id

Keywords:SAR, Surface Manifestation, Geothermal, Backscattering, Remote Sensing.

ABSTRACT

The optical remote sensing sensors were facing problem to identify ground surface under Torrid Zone for last decades. The cloud and thick vegetation canopy always becomes an obstacle for remotely sensed sensor to reveal surface geology features. Therefore, the advantage of satellite data for geology exploration as well as hazard mitigation is less effective. Nowadays, remote sensing technology is approaching a new era, especially in the use of microwave sensors onboard space borne termed as Synthetic Aperture Radar (SAR). The SAR is an active remote sensing technology which operates regardless time and weather condition. The application of SAR sensor for geology and geothermal related study is growing rapidly. However, the use of backscattering intensity of SAR data for geothermal prospection is still limited. The main problem might be originated from the geometric distortion and/or limitation of waveband. Overcoming the problem, we present our achievements in the use of backscattering intensity of SAR data for detecting surface manifestation precisely. An automatic extraction of linear feature density from Synthetic Aperture Radar (lifedSAR) is demonstrated to estimate the fluid path related to faults and fractures at Mt. TangkubanParahu, West Java, Indonesia. In addition, a Polarimetric SAR data was used to detect the distribution of surface manifestation based on surface roughness criterion. Combining both methods is superior to minimize the detection errors from environment noises. Following this approach, we could correlate the surface manifestation with Linear Features Density (LFD) and surface roughness. The alteration zones are located at medium to high LFD values and low to medium surface roughness, respectively. The Fluid Path Index (FPI) and field investigation confirmed the location of alteration zones in the SAR backscattering image. Therefore, detection accuracy using remotely sensed data under Torrid Zone could be improved as presented in this study.

1. INTRODUCTION

The atmospheric disturbances prevent the optical sensor to detect surface geology correctly. The Synthetic Aperture Radar (SAR) as an active remote sensing utilized in the microwave region is superior to detect physical properties of ground surface such as surface roughness and soil moisture regardless atmospheric condition. Alonger wavelength is plausible for deeper target detection for example the L-band (=23.6 cm) has possibility to penetrate the clouds and dry ground surfaces (Kozlov et al., 2001). These advantageous meet the needs of surface geology characterization under Torrid Zone, such as in Indonesia. In this paper, we used the SAR power return or backscattering intensity data from the Phased Array L-band Synthetic Aperture Radar (PALSAR) onboard the Advanced Land Observing Satellite (ALOS) to characterize surface manifestation of geothermal system.The ALOS PALSAR was developed by Japanese Ministry of Economy, Trade and Industry (METI) as a joint project with Japan Aerospace Exploration Agency (JAXA) and launched from Tanegashima Space Center. Contrary to the X- and C-bands, the L-band enables to penetrate the clouds and reduce the effects of canopy vegetation (Henderson and Lewis, 1998). There are two SAR data types used in this study: (1) single and (2) quad (full) polarization types. For single polarization data, we used dual orbit observation in Ascending (satellite orbits toward North) and Descending (satellite orbits toward South). The ALOS PALSAR data level 1.5 in multilook geocoded are used as basis for ground surface characterizations. Detail data used are listed in Table 1. Mt. Tangkuban Parahu termed as MTP in West Java, Indonesia was selected as study site due to existence of several surface manifestations such as alteration zones and hot springs. Thus, validation could be performed by field investigation. The MTP is an active volcano composed by complex geological history (Figure 1). This volcano is the youngest system of the great Sunda Caldera volcanism. The volcanism at MTP was evolved from two caldera systems: (1) 200.000 and (2) 90.000 years ago (Kartadinata, 2005). Following Kartadinata (2005), volcanism of MTP was composed by two volcanic activities: (1) the Old and (2) Young MTP which is dated about more and less than 10.000 years ago, respectively. The Old Tangkuban Parahu termed as OTP is characterized by large catastrophic which produced about 30 different rock types. The tephra-chronology indicated that the OTP is composed by stratification of phreato-magmatic and magmatic volcanic products. The phreato-magmatic volcanic products are characterized by dark to bright volcanic ashes, lamination structure, vesicles, and accretion of lapilli. On the other hand, the magmatic volcanic products are identified by interchange of stratification between scoriae and volcanic ashes. Instead of scoriae and volcanic ashes, the magmatic eruption also produced andesitic and basaltic lava flow deposits (Sunardi and Kimura, 1998). The Young MTP termed as YTP is composed by 12 different rock types which is produced by phreatic eruption. Among the 12 rock types, there are dark vesicular-scoriae from the latest magmatic eruption in 1910. The eruption in 1910 is interpreted as the last magmatic eruption of MTP. The later activity is characterized by short phreatic eruptions and hydrothermal activity (Sumaryadi et al., 2011).

Table 1. Details ALOS PALSAR data used in this study.

No	Data Type	Orbit	Date
1	Single Polarization	Ascending	4 December 2008
2	Single Polarization	Descending	13 December 2008
3	Full Polarization	Ascending	4 June 2010

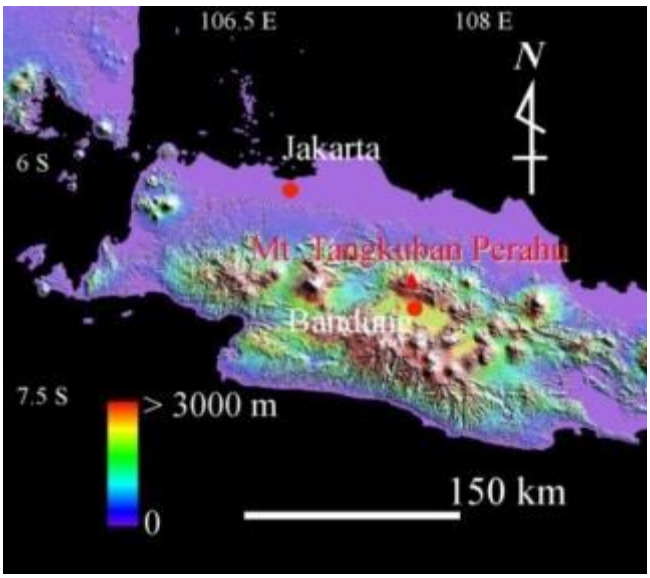

Figure1: Location of Mt. Tangkuban Parahu (MTP) pointed by red triangle and overlaid on the elevation map (Sumintadireja et al., 2013).

2. DUAL SAR OBSERVATIONS FOR FLUID PATH DETECTION

The SARsensor observes ground surface at off nadir, thus there is an angle of look between the sensor and target. The angle of look produces ground surface image in the Line of Sight (LOS) direction or slant range. The slant range image caused the geometrical distortion of the ground and lost information especially at mountainous terrain due to foreshortening and shadowing effects. Overcoming the problem, we used a dual SAR data orbits in opposite LOS (Ascending and Descending) to compensate the distortion and lost information. Figure 2 shows the SAR backscattering intensity images of MTP in Ascending and Descending modes. Using SAR backscattering intensity data, the Geomorphologic and Structural features (GSF) could be detected in detail (Saepuloh et al., 2012a). The two orbits provided visual GSF in opposite point of view satellite. The slope facing toward the sensor will be brighter than backward due to strong backscattering return to the receiver. The back-slope might be dark due to weak signal return to the receiver. The use of dual orbits is effective to reduce the weak signal in the SAR imagery. Moreover, the backscattering intensity of high topography or mountainous terrain will be higher than flat terrain. The high contrast between high and low topography is superior for detection purposes of the linear features related to geological structures. The linear features according to the GSF in the SAR imagery are crucial for predicting the fluid path of geothermal system at ground surface. The features are characterized generally by contrast tone of the ridges, valleys, hills, and rivers. Following Saepuloh et al.(2012b), we applied an automatic extraction of linear feature density from Synthetic Aperture Radar (lifedSAR) to quantify linear features of dual SAR orbits.

(A) (B)

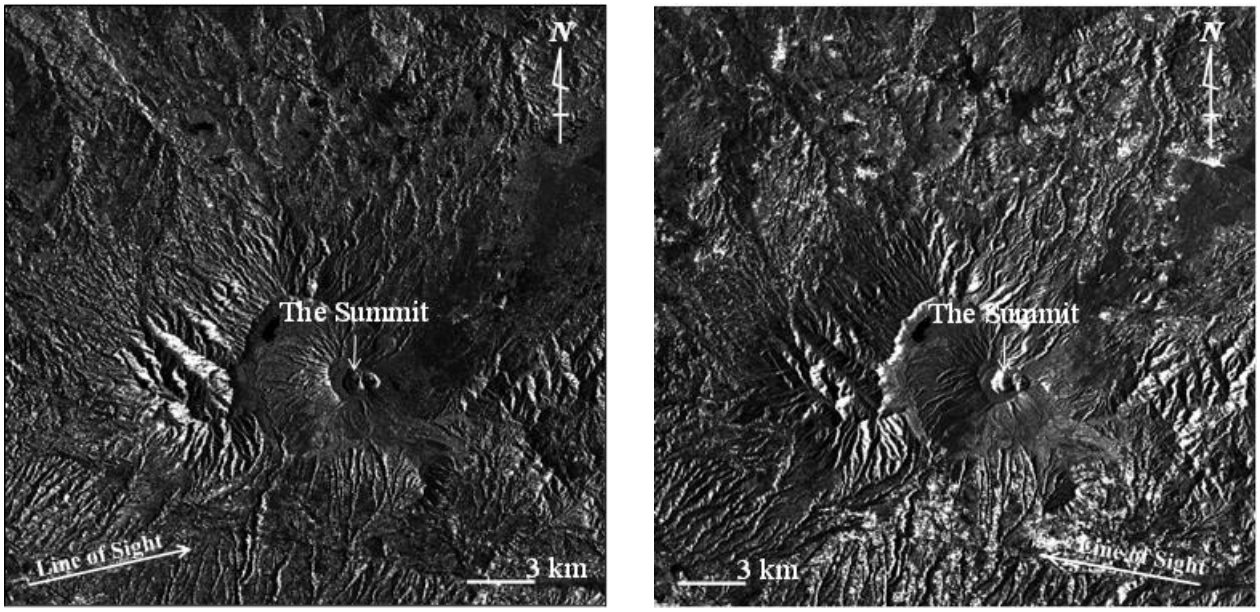

Figure 2: Backscattering intensities of ALOS PALSAR data in Ascending (A) and Descending (B) orbits show MTP at West and East Line of Sight (LOS). The circular geomorphologic feature at the summit is a crater lake of MTP.

The image processing and lifedSAR work flows are discussed as follows. The ALOS PALSAR level 1.0 data were calibrated into level 1.1 data or Single Look Complex (SLC). The level 1.1 data were then quantified by a multi-look processing with 3×6 factor to keep the spatial resolution of image along the range and azimuth directions as 28 m and 23 m, respectively. The multi-look image in slant range coordinate was transformed to ground range based on simulated-DEM derived from the SRTM 90 m data. The processing result is a multi-looked and geocoded data in level 1.5. The ALOS PALSAR data were provided by Jspacesystem using ASTER/ALOS unified seach web interface (http://gds.ersdac.jspacesystems.or.jp/). The ALOS PALSAR level 1.5 were used as input of lifedSAR. The first step of the lifedSAR is an edge detection process. The process is applied to delineate discontinuity of pixel brightness. Then, the detetced edges are organized into a curved line segments. This standards edge detection process caused a problem due to geometrical distortions in the SAR imagery. The high gradient topography produced double edges at back- and fore-slope in the SAR backscattering intensity images. Overcoming the problem, we selected only the fore-slope for calculation because of various geomorphologic features. The Laplacian of Gaussian (LoG) filter was incorporated by lifedSAR to detect the edge of GSF presented in backscattering intensity images. The LoG filter is superior to minimize loss information and decrease processing time (Sotak and Boyer, 1989). To simplify calculation, a binarization process was adopted following the LoG filtering. Then, the Linear Features Density (LFD) could be calculated based on binary image at 10×10 window size as follows:

$$LFD = \sum_{n=1}^{w} \left[A_n(x,y) \right]_{Q75} \Delta P \tag{1}$$

where w is windows size, A is pixel number of linear features, $Q75$ is a selected threshold using the 3rd quartile of the histogram of backscattering intensity images, and Δp is pixel resolution. The 10×10 window size is an optimum for image size 800×800 (=40×40 km). The window size out from 10×10 would produce the contour map of LFD unrealistic to the geological structures at field scale (Saepuloh et al., 2012b). A high frequency filtering was then applied to remove uncorrelated features.

To confirm the correctness of the lifedSAR, we extracted the GSF including circular pattern of the crater rims and geological structures. The extractions were performed based on visual interpretation of the backscattering intensity images to find the correct GSF. Then, detected GSF and lifedSAR results are overlaid and depicted in Figure 3. Simply, the LFD values less than 0.4% and higher than 0.7% are classified to low and high density, respectively. The maximum densities more than 0.7% are located at S, NW, and NE flanks from the summit. The locations agree to the location of faults and/or crater rims. The maximum density at S coincides to the location of the great Lembang Fault. The fault bordered the MTP volcanic products at the South. The high LFD values at NW and NE agree to the faults and old crater rims of OTP volcanic activity. There are two interesting phenomena could be detected and discussed as follows. The minimum LFD values at NE from the summit agree to the new volcanic products of YTP. The products are composed by pyroclastic and lava flows which are deposited toward the NE from the summit. Another phenomenon could be detected that the location of surface manifestations agrees to the medium to high LFD values. This phenomena is extraordinary because the surface manifestation from discharge area are usually located at faults and fractures zones with maximum to high LFD values (Saepuloh et al., 2012b). However, the surface manifestation at MTP are located at medium to high LFD values.

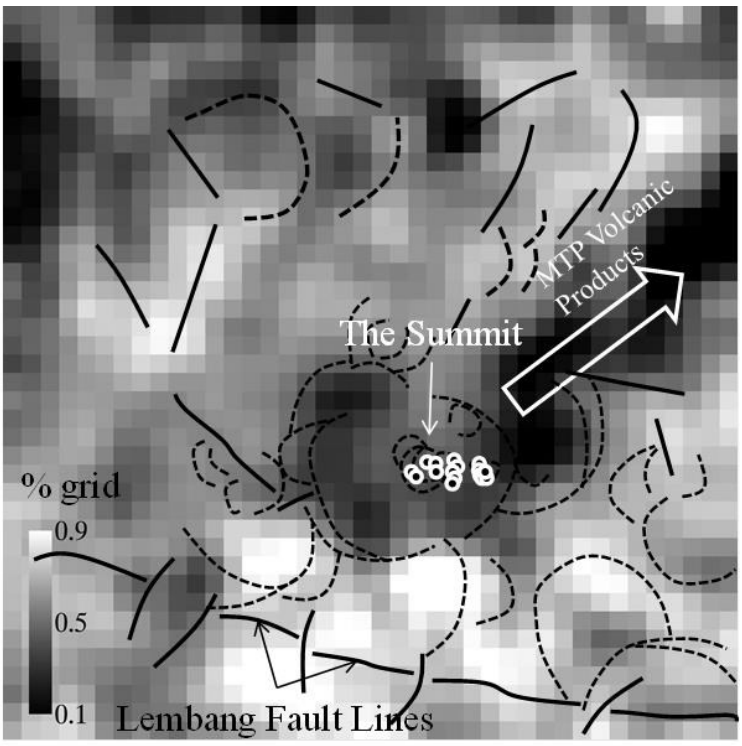

Figure 3: Surface manifestations (black dots) around the summit of MTP overlaid on the Linear Features Density (LFD) from dual observations of ALOS PALSAR data as shown by Figure 3. Dashed lines are complex craters, black lines are main interpreted faults, and large arrow is direction of MTP volcanic products toward NE.

3. SURFACE MANIFESTATION ON POLARIMETRIC SAR DATA

Contrary to the optical sensors with their multispectral wavelength or wavebands capability, the SAR sensors generally operate only at single wavelength channel so that the surface characterization is more complicated. Overcoming the problem, some SAR sensors such as ALOS PALSAR are utilized by polarization mode. Simply, the electromagnetic signal from transmitter and receiver could be filtered into two components: (1) Vertical and (2) Horizontal termed as V and H, respectively. When the SAR sensor transmit the H component and receive the V component, then the HV data type will be produced. Therefore, the sensor produces four combination data types for each acquisition time: (1) HH, (2) HV, (3) VH, and (4) VV. The four data combinations are termed as quad or full-polarimetric data.We useda full-polarimetric of ALOS PALSAR data to characterize surface manifestation (Figure 4A). The geomorphologic features of the summit craters could be detected clearly by pink and dark tonal. The valleys and rivers are also presented by dark tonal with radial pattern from the summit toward foot of volcano. Based on the GSF of full-polarized data, the MTP are composed by twelve different volcanic rocks (Saepuloh et al., 2012c). The MTP volcanic rocks are composed by pyroclastic falls, lava flows, basaltic lavas, pyroclastic flows, and lava cone deposits.

To detect the surface roughness, we used the HV polarization mode because of its sensitivity to surface roughness associated with volcanic products (Kozlov et al., 2001). In view point of GSF, the surface roughness might be represent the response of surface materials to the erosion, weathering, or alteration processess. For this study, the alteration process is the key point for estimation the geothermal system beneath the surface. The ground surface of altered rocks is interpreted smoother than fresh rocks due to contact with geothermal fluids. Therefore, we modified the surface roughness extraction from Campbell and Shepard (1996) using HV and VV polarization types. The surface roughness, R_0, was calculated as follows:

$$R_0 = 10 \times \left[\lambda \sqrt{\left|-\frac{1}{60}\ln\left(-\frac{f(\sigma_{HV},\sigma_{VV})}{0.04\times\cos\theta_i}\right)\right|}\right] \times \sin\theta_i \quad (2)$$

where λ is wavelength, $f(\sigma_{HV}, \sigma_{VV})$ is backscattering intensity as function of cross- and co-polarized types, and θ_i is local incidence angle.

The roughness degree is presented by Root Mean Square (RMS) in m unit. The surface roughness depends on the wavelength used by the sensor so that 23.6 cm is basis of roughness criterion using ALOS PALSAR data (Anugrah et al., 2014). The R_0 image is depicted in Figure 4B. In general, the surface roughness at Northern flank is higher than Southern flank. The new MTP volcanic products are interpreted responsible to the high surface roughness. The fresh volcanic products usually have rough surface due to weak erosion process. The surface roughness of Baru and Domas Crater rim shows high, but the Ratu Crater rim shows low. Based on field investigation, there are eight locations of altered zones around Ratu Crater rim, seven locations around Baru Crater rim, and eight locations around Domas Crater rim. Generaly, the alteration rocks are located at low surface roughness except at the Domas Crater and Southern part of Ratu Crater at medium surface roughness (see Figure 4B).

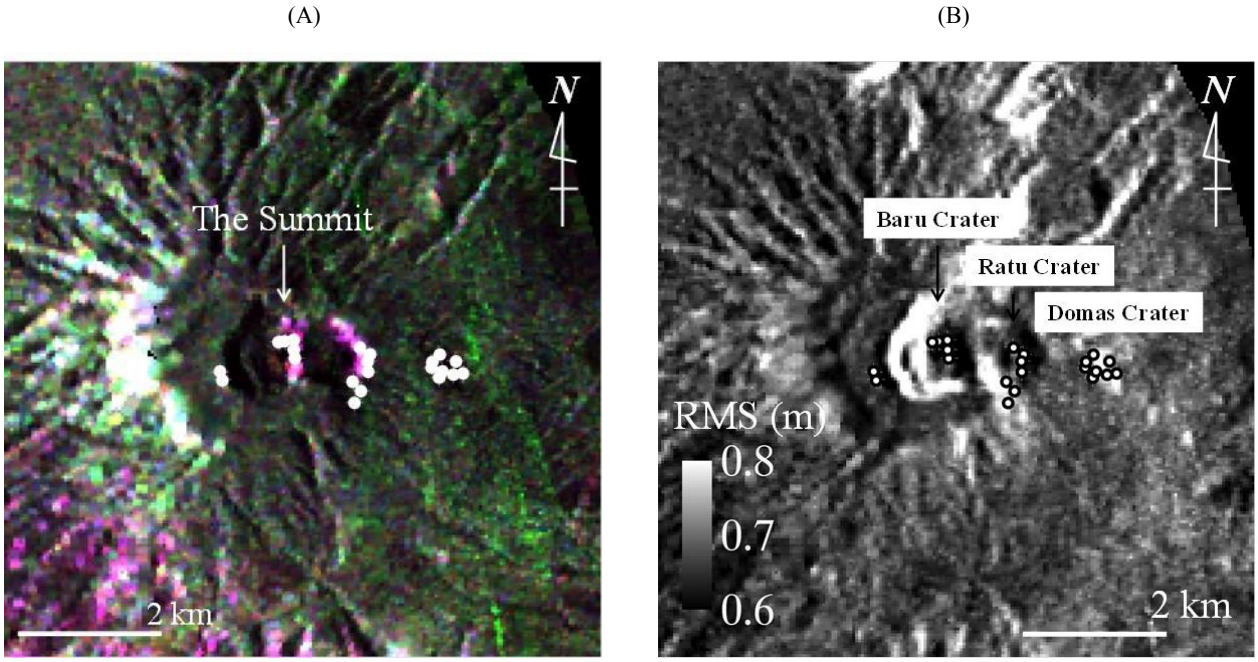

Figure 4: (A) Surface manifestations (white dots) arround the summit of MTP overlaid on the backscatter intensity image of ALOS PALSAR polarimetric data. The image is presented by color composite of R, G, B = HH, HV, VV and (B) Surface roughness model generated from HV and VV polarization types shows that surface manifestations are located at low to medium surface roughness.

4. RESULT AND DISCUSSION

There are two ground surface parameters could be extracted successfully using SAR backscattering intensity images termed as Linear Features Density (LFD) and surface roughness (R_o). The two parameters could be used to detect the surface manifestation especially the alteration zones of a geothermal system. In order to understand the response of altered rocks to the SAR backscattering intensity, we correlated the LFD to the R_o (Figure 5A). Based on this cross-correlation plot, the LFD has an opposite correlation to the R_o. It may infer that the alteration zones are located at high LFD or dense linear features with low R_o or smooth surfaces. High LFD located at high fractured zones where the hydrothermal fluid could reach to the surface. The fractured zones served as fluid path of geothermal system by the means. On the other hand, the location of alteration zones at smooth surface could be interpreted that the contact between hydrothermal fluids and rocks or formations caused the ground surface smoother than fresh rocks. The alteration among the minerals might cause a weakening of molecular bonds. Therefore, the rock surface could be decomposed and produced smooth surfaces. Following this consideration, we targetted the location with dense linear features and smooth surface as fluid path of hydrothermal system. The fluid paths is crucial for a geohermal exploration becauase they could serve as the key to predict the alteration or high permeability zones . In order to predict the fluid paths susing LFD and R_o parameters, we calculated the Fluid Paths Index, *FPI*, as follows:

$$\mathrm{FPI} = \frac{(\mathrm{LFD} - \mathrm{R_0})}{(\mathrm{LFD} + \mathrm{R_0})} \tag{3}$$

where *FPI* is fluid path index, *LFD* and R_0 are linear features density (% grid) and RMS surface roughness (cm), respectively.

The cross-correlation between *LFD* and *FPI* has a positive gradient slope and linear correlation with R^2 value almost one (Figure 5B). The positive gradient slope is used as basis to select the *FPI* as the most plausible parameter for fluid path detections of a geothermal system.The calculation result of *FPI* is depicted in Figure 6. The color scale from blue to red indicates the low and high *FPI* values, respectively. The maximum *FPI* values are located at North and South flanks from the summit. The minimum *FPI* values are located at NW and NE flanks, respectively. The minimum values at NE flank caused by zero R_0 due to out of scene data (see Figure 4B). The medium FPI values presented by green portion are located around the summit craters of MTP. The white dots are location of altered zones and the white dashed curves are *FPI* delineation. An interesting phenomenon could be seen that the altered zones are located at medium *FPI* presented by green portion. Based on the cross-correlation plot in Figure 5B, the surface manifestations are predicted at high *FPI* generally. Therefore, this condition could be interpreted as follows. Based on field observation, the altered zones are located around the summit craters (see Figure 4A). The geomorphologic of the craters are identified by high relief topography and deep valleys. In view point of geothermal system, the geomorphologic features at the summit are identical for the upflow zones that the hydrothermal fluid ascents to the surface. The volcanic rocks around the upflow zones could be altered due to contact with hydrothermal fluids. The upflow zones might be also composed by alteration rocks. Therefore, the surface manifestations could be detected at outflow and upflow zones.

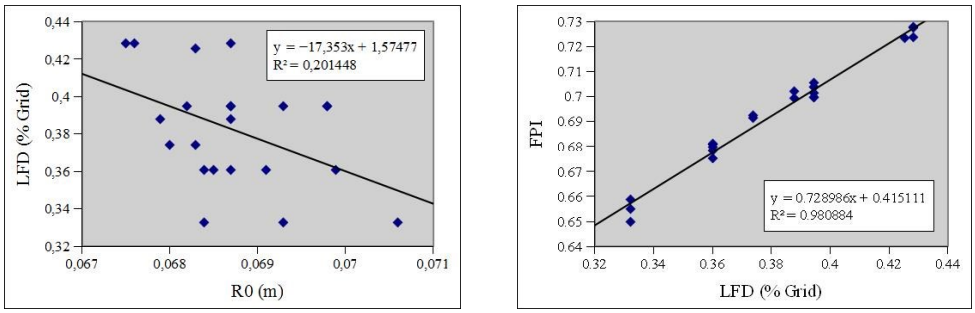

Figure 5: (Left) The correlation plots between LFD to R_0 and (Right) *FPI* show negative and positive gradient slopes, respectively. The positive gradient slope is used as basis to select the *FPI* as the most plausible parameter for fluid path detections of a geothermal system.

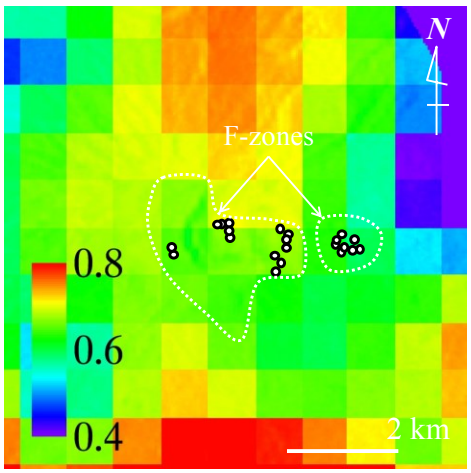

Figure 6: The fluid path zones termed as F-zones were detected using Fluid Path Index (*FPI*) from RMS surface roughness and LFD from ALOS PALSAR backscattering intensity data.

Classifying the alteration zones from outflow or upflow zones using SAR remotely sensed data is a complicated task because of limitation of spectral bands. However, in this study we could detect the alteration zones at upflow zone using fluid path criterion (*FPI)*. The fluid paths termed as F-zones are located around the upflow zones at MTP (Figure 6).The ground surface around the upflow zones are characterized by medium to high *LFD* (=0.75), low to medium R_0 (=0.6), and medium *FPI* (=0.6). These three parameters are potential for defining surface manifestations from upflow zones. On the other hand, the high *FPI* values at Southern flank probably originated from the Lembang Fault (see Figure 3). The high relief topography of the large fault surfaces is also presented by high *FPI* values. The fault system migh serve as recharge area of the hydothermal system beneath MTP. In addition, the high *FPI* values at Northern flank might serve as discharge area due to hydrothermal fluid circulation toward the lower topography at the South. This interpretation is confirmed by the existence of hot spring zones at about 10 km at North from the summit. Further field investigation at the high *FPI* values at Northern and Southern flanks from the summit crater are the next step to this study.

5. CONCLUSION

The SAR backscattering intensity data from dual orbits mode proved effective to quantify structural features at ground surface in opposite Line of Sight (LOS) satellite. The geometric distortion problem in the SAR data could be minimized by combining two different satellite orbits: Ascending and Descending.The structural features presented in linear features in the SAR backscattering images served as a key to predict the fluid paths of a geothermal system. Based on the automatic extraction of linear feature density from SAR (lifedSAR), the minimum LFD values at NE from the MTP summit agree to the new volcanic products. The products are composed by pyroclastic and lava flows which are deposited toward the NE from the summit. Another phenomenon could be detected that the locations of surface manifestations agree to the medium to high LFD values. The surface roughness could be used as parameter to classify surface manifestation zones. For MTP, the surface roughness at Northern flank associated to the new MTP volcanic products. The roughness degree at Northern flank is higher than Southern flank. For the summit craters, The surface roughness at Baru and Domas Crater rims is higher than Ratu Crater rim. The alteration zones are located at low to medium surface roughness around the three craters. The alteration zones at upflow zone could be characterized using fluid path criterion. The fluid paths termed as F-zones are located around the upflow zones at the summit craters. The altered ground surface around the up flow zones are characterized by medium-high Linear Features Density (LFD), low-medium surface roughness (R_0), and medium FPI. In addition, the high FPI values at Southern and Northern flanks which are predicted as recharge and and discharge area due to hydrothermal fluid circulation from South toward North.

ACKNOWLEDGEMENT

The ALOS PALSAR data used in this study are provided by Japan Space System, formerly Earth Remote Sensing Data Analysis Center (ERSDAC), Japan. The authors thank to Mr. Afy for his effort collecting alteration rocks at MTP during field investigation in March 2014.

REFERENCES

Anugrah F.A., Saepuloh A., Wikantika A., Surface Roughness Modeling using Polarimetric SAR Data to Delineate Geomorphologic of Mineralization Zones at Volcanic Terrain, *Proceedings of the Asian Conference on Remote Sensing 2014*, Paper No. PS-043, Nay Pyi Taw, Myanmar (2014).

Campbell, B. A. and Shepard, M. K.: Lava flow surface roughness and depolarized radar scattering, *Journal of Geophysical Research*, **101**, (1996), 18941–18951.

Henderson, M.and Lewis, J.:*Principles and applications of imaging radar*. New York: John Wiley & Sons Inc., ch. 5, (1998), 271-356.

Kartadinata, M.N.: Tephrochronological Study on Erup-tive History of Sunda-Tangkuban Parahu Volcanic Com-plex, West Java, Indonesia, *A doctoral dissertation, Nature System Science*, Graduate School of Science and Engineering, Kagoshima University, Japan (2005).

Kozlov, A.I., Lighthart, L.P., and Logvin A.I.: *Mathematical and Physical Modelling of Microwave Scattering and Polarimetric Remote Sensing*, Kluwer Academic Publisher, Netherland (2001).

Saepuloh, A., Koike, K., and Omura, M.: Applying bayesian decision classification to Pi-SAR polarimetric data for detailed extraction of the geomorphologic and structural features of an active volcano, *IEEE-GRSL*, (2012a), 1-5.

Saepuloh, A., Urai, M., Meilano, I., and Sumintadireja, P.: Automatic extraction and validation of linear features density from ALOS PALSAR data for active faults and volcanoes, *Proceedings of the International Symposium on Remote Sensing*, Chiba, Japan (2012b).

Saepuloh A., Urai M., Bayuaji L., Sumintadireja P., Suparka E.: Identifying volcanic rocks using geomorphologic and structural features of polarimetric SAR data, *Proceedings of the 5th Indonesia-Japan Joint Scientific Symposium (IJJS)*, Chiba-University, Japan (2012c).

Sotak, G.E. and Boyer, K.L.: The Laplacian-of-Gaussian kernel: a formal analysis and design procedure for fast, accurate convolution and full-frame output, *Computer Vision, Graphics, and Image Processing*, **48**, (1989), 147-189.

Sumintadireja P, Subroto E.A., Saepuloh A, Urai M., Takada A.: The Importance of Continuous Research for Mitigating and Monitoring Volcanic Activity at Mt. TangkubanParahu, *Proceeding of the 1st International Seminar of Environmental Geosciences in Asia (1st ISEGA)*, ITB, Bandung, (2013), 90-94.